JOURNAL OF VIROLOGY, June 1986, p. 970–974
0022-538X/86/060970-05$02.00/0

Vol. 58, No. 3

Nuclease Mechanism of the Avian Retrovirus pp32 Endonuclease

DUANE P. GRANDGENETT,[1]* AJAYKUMAR C. VORA,[1] RONALD SWANSTROM,[2] AND JOHN C. OLSEN[2]

Institute for Molecular Virology, Saint Louis University Medical Center, St. Louis, Missouri 63110,[1] and Department of Biochemistry and Lineberger Cancer Research Center, University of North Carolina, Chapel Hill, North Carolina 27512[2]

Received 20 December 1985/Accepted 10 March 1986

In vivo, the inferred circular retrovirus DNA precursor to the provirus contains two long terminal repeats (LTRs) in tandem. We studied the site-specific nicking of supercoiled DNA that contains tandem copies of avian retrovirus LTR DNA in vitro by using purified avian myeloblastosis virus pp32 endonuclease, Mg^{2+}, and viral DNA substrates containing different LTR circle junction sequences. The results confirmed our previous observation that the pp32 protein generates two nicks, one in either viral DNA strand, each 2 nucleotides from the circle junction site. The specificity of nicking by pp32 was unchanged over an eight-fold range of protein concentration and with different avian retrovirus LTR circle junction substrates. These data are consistent with models which propose a role for the endonuclease in removal of two nucleotides from the LTR termini on integration of viral DNA in vivo.

Integration by retroviruses requires a virus-coded function. A DNA endonuclease, termed pp32 with a molecular weight of 32,000, is encoded in the 3'-terminal one-third of the avian retrovirus polymerase gene, *pol* (2, 6, 10). Several avian retrovirus *pol* mutants exhibit DNA endonuclease defects only in the presence of polymerase and RNase H defects, thereby preventing evaluation of the endonuclease function(s) per se in the integration reaction in vivo (8). Site-directed mutagenesis of cloned murine leukemia retrovirus DNA (3, 23) and spleen necrosis virus DNA (19) has established that the putative endonuclease coding domain at the 3' terminus of *pol* in these viruses is required for integration. Analysis of frameshift mutations, small deletions, and point mutations in the pp32 DNA endonuclease-DNA binding domain of an avian retrovirus, the Prague A strain of Rous sarcoma virus, suggests that this region also encodes other undefined function(s) besides integration (11, 12).

The partially phosphorylated pp32 protein (22) possesses DNA-nicking activity in the presence of Mg^{2+} or Mn^{2+} (10). Mn^{2+}-dependent DNA nicking activity (7, 14, 21) is also found with the parental molecule of pp32, the 92,000-dalton β polypeptide (2, 6, 10). The Mn^{2+}-dependent DNA-nicking activity associated with αβ DNA polymerase is able to cleave either the plus or the minus strand of avian retrovirus DNA in the region of the long terminal repeat (LTR) circle junction site, resulting in one nick per molecule, each mapping 3 nucleotides from the circle junction (4, 5, 24). Avian myeloblastosis virus (AMV) pp32 endonuclease in the presence of Mg^{2+} preferentially nicks supercoiled DNA containing the avian retrovirus LTR circle junction sequences at either one or the other of two sites, each of which mapped 2 nucleotides back from the circle junction (9) (Fig. 1). In this study, we further characterized the nicking of the LTR circle junction by pp32 by using various assay conditions and LTR DNA substrates. The results of these studies support a role for pp32 DNA endonuclease in integration.

Effect of varying pp32 protein concentrations on nicking near the LTR circle junction. The pp32 protein apparently forms a nucleosomelike structure in the LTR circle junction region (13, 16); the area covered starts about 135 nucleotides upstream of the circle junction site (R200) and ends 34 nucleotides downstream of the circle junction site. The binding of pp32 to this region was detected by DNase I nuclease protection experiments which were performed at relatively high protein-to-DNA molar ratios (~100:1). We wanted to define the relative frequencies of cleavage at the four major nicked sites generated by pp32 in the circle junction region over an eightfold protein concentration (Fig. 2, 3, and 4). Supercoiled pPvuII-DG was nicked by pp32 at protein-DNA molar ratios of 11:1, 22:1, 33:1, and 44:1 (Fig. 2 and 3, lanes 2, 3, 4, and 5, respectively). The percents conversion of supercoiled to nicked circles were approximately 5, 10, 15, and 25%, respectively (data not shown). Only two DNA fragments generated by pp32 comigrating with markers (15) at R329 and L39 are evident. Therefore, by interpretation, the endonuclease generates nicks at R328 or L38, respectively (Fig. 1 and 2). Quantitation by densitometer tracings in the linear response range of several exposed gels demonstrated that the ratio of nicks at R328 to those at L38 was approximately 0.7 ± 0.2. Apparently, the pp32 protein cleaves these two sites at nearly equivalent frequencies under these assay conditions. Longer exposure of the gel shown in Fig. 2 also demonstrated that, at the higher pp32 protein concentrations (lanes 4 and 5), the endonuclease was capable of introducing another nick at R327, although much less frequently compared with nicking at R328. With Mn^{2+} present, nicking at R327 occurs two times more frequently than at R328 (9).

The data in Fig. 3 (lanes 2 and 3) show that pp32 was capable of preferentially generating nicks at L2 and L23 on the minus viral strand at lower protein-DNA molar ratios (Fig. 1). However, higher protein concentrations produced major nicks at L41, L42, L51, and L55. Longer exposure of the gel in Fig. 3 demonstrated nicking at L3.

Frequency of nicking on plus and minus strands. Direct comparison of the frequencies of nicks on the plus and minus strands was possible by 5' end labeling both ends of the 330-base-pair (bp) *Eco*RI LTR fragment (Fig. 1) and simultaneously analyzing the sites of nicking on both strands (Fig. 4, lane 1). It was possible to identify all four major nicked sites generated by pp32. Subsequent digestion of the 330-bp fragment with *Hin*fI, which shortens the labeled plus-strand fragment (Fig. 1), clearly identified the two fragments (L2

* Corresponding author.

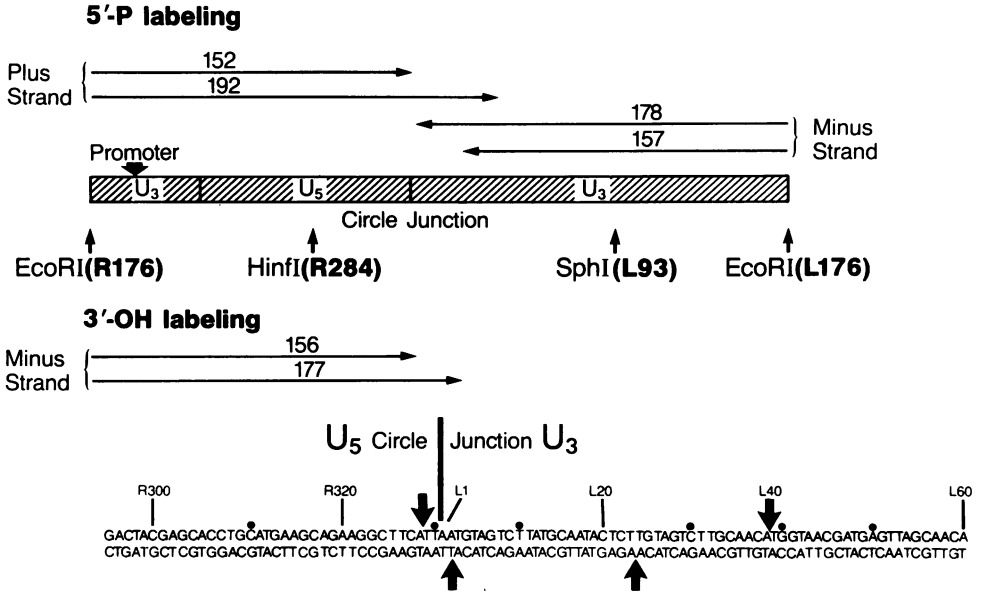

FIG. 1. Scheme for identifying AMV pp32-nicked sites in the avian retrovirus LTR DNA circle junction region. The shaded area represents the LTR region in pPvuII-DG between the *Eco*RI sites of the tandem LTRs. The 330-bp *Eco*RI fragment was 5′ end labeled with [γ^{32}P]ATP and polynucleotide kinase. This doubly end-labeled fragment was either analyzed directly or cleaved with an appropriate restriction enzyme to define the orientation of the nicked sites. *Hin*fI or *Sph*I digestion of the 330-bp fragment results in generation of a 223- or 247-bp uniquely labeled fragment, respectively. For 3′ end labeling, the samples were digested with *Eco*RI and *Sph*I prior to labeling at the *Eco*RI site with [α^{32}P]dATP in a fill-in reaction with DNA polymerase. The horizontal arrows indicate the lengths of the labeled single-stranded DNA fragments resulting from the major nicked sites generated by pp32, and the sites of these nicks are indicated on the sequence by vertical arrows (9). The viral plus and minus LTR DNA sequences (top and bottom, respectively) which are located on either side of the circle junction site are shown. Numbers with the prefix R refer to the positions of sequences within the LTR adjacent to the v-*src* region on the right end of the linear map of unintegrated viral DNA. Numbers with the prefix L refer to the position of sequences within the LTR adjacent to the *gag* region on the left end of the linear map; in both cases, position 1 is at the leftward boundary of U_3 (26).

and L23) that were generated as a result of cleavage on the minus strand (Fig. 4, lane 2). The largest fragment (192 nucleotides in length; lane 1) and the smallest fragment (152 nucleotides in length; lane 1) are the results of nicks introduced in the viral plus strands at L38 and R328, respectively, since these fragments are lost after cleavage with *Hin*fI (Fig. 4; compare lanes 1 and 2). The nick at R328 occurred at a frequency 0.7 times that of the nick at L38. In contrast, the frequency of nicking on the minus strand at L2 compared with L23 occurred at a ratio of 1.7.

One additional comparison was made: the frequency of nicking at R328 on the plus strand and L2 on the minus strand, each site 2 nucleotides away from the circle junction site (Fig. 4, lane 1). The pp32 endonuclease nicked two times more frequently at L2 than at R328.

Comparison of different LTR DNA circle junction substrates. The circle junction of Rous-associated virus type 2 (RAV-2) (4, 24) was utilized as the substrate for pp32 endonuclease in the presence of Mg^{2+}. There are several substitutions and insertions in the RAV-2 U_3 region compared with the Schmidt-Ruppin A RSV sequence (26). The cloned RAV-2 LTR DNA (supplied by A. Skalka) used in the assay consisted only of sequences between the LTR *Eco*RI sites (Fig. 1) in contrast to the pPvuII-DG clone, which also contained some v-*src* and *gag* sequences (26). The pp32 endonuclease generated only four nicked sites on the RAV-2 LTR DNA which map to the identical positions as shown for Schmidt-Ruppin A LTR DNA (Fig. 1; data not shown).

Replacement of the immediate (35 bp) circle junction sequences in a DNA clone containing tandem copies of the PrA Rous sarcoma virus LTR sequence with a 25-bp DNA fragment containing sequences of the viral plus-strand primer-binding site resulted in inability of the pp32 protein to protect this region from DNase I digestion, although other LTR DNA sequences (R175 to R260; Fig. 1) were protected (16). The 35-bp deletion-insertion at the circle junction site mapped from R319 through the circle junction to L22 (Fig. 1). The DNA clone (pXBM-102) containing these incomplete tandem LTRs was nicked by pp32 in the presence of Mg^{2+} at several different protein-DNA molar ratios (25:1 and 50:1). The percents conversion of supercoiled DNA to nicked circles were approximately 5 and 10%, respectively. The pp32 protein did not nick within the LTR region on either strand between R250 and L59 (data not shown). Only one nick site (L60) on the viral plus strand was observed, but only weakly. These data suggest that the sequence at the circle junction site plays an important function in the cleavage reaction as previously demonstrated for the integration reaction in vivo (1, 18).

A Schmidt-Ruppin A Rous sarcoma virus DNA clone (pA043) with an altered circle junction site was also tested in the nicking assay. This clone has an extra dA-dT base pair inserted at the circle junction site, resulting in the sequence of CATT-AAATG (17). The additional dA was numbered L3 in pA043, thus resulting in an increase of one for all nucleotides in U_3 compared with pPvuII-DG. We wanted to determine whether pp32 was still capable of nicking at the conserved CA (R328, plus strand) and AC (L2, minus strand) dinucleotides even with an additional nucleotide between the conserved dinucleotides. pA043 DNA was nicked by pp32 and digested with *Eco*RI, and the 331-bp DNA fragment was 5′ end labeled. To determine whether pp32 nicked at L2 or L3 on the minus strand, the *Eco*RI fragment was digested with *Hin*fI, and the resulting 224-bp fragment was analyzed.

The highest-molecular-weight fragment generated by pp32 comigrated with the size marker at position L3 (Fig. 5, lanes 3, 4, and 5), in contrast to the cleavage of pPvuII-DG (Fig. 4) or RAV-2 (data not shown), where the DNA fragment generated by pp32 comigrated with the size marker at position L2. In all cases, the pp32 protein nicked the minus strand at the conserved AC dinucleotide. The additional cleavage seen in this region using pPvuII-DG as the substrate was also seen using pA043 (at L24 on the pA043 map).

Further analysis of pA043 nicked by pp32 demonstrated that the plus strand was cleaved at R328 and L39 (data not shown). These results were confirmed by examination of the 331-bp end-labeled *Eco*RI fragment from pA043 (Fig. 5, lanes 1 and 2). The DNA fragment comigrating at R317 (lane 2; 193 nucleotides long) mapped to L38 (AACA ↓ T) on the plus strand of pPvuII-DG or L39 on the plus strand of pA043. The faint DNA fragment in lane 2 (152 nucleotides long) comigrating at L29 on the minus strand mapped to R328 on the plus strand of pPvuII-DG or pA043. It should be noted that pp32 again nicked at L3 on the minus strand at a considerably higher frequency than at R328 on the plus strand. Several other nicks observed on the *Eco*RI 331-bp fragment (Fig. 5, lane 2) mapped to the minus strand at L37 and L41. Thus, pp32 nicked at the conserved CA dinucleotide adjacent to the circle junction site with either pA043, pPvuII-DG, or RAV-2.

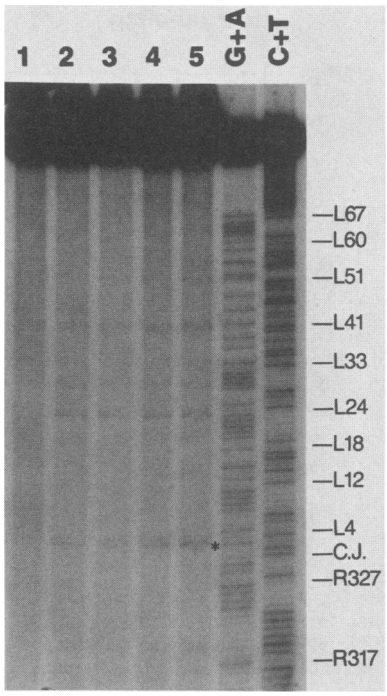

FIG. 3. Effect of varying AMV pp32 concentration on nicking within the Schmidt-Ruppin A LTR region viral minus strand. The DNA nicking conditions were as described in the legend to Fig. 2. One-half of the sample was digested with *Eco*RI and *Sph*I and 3′ end labeled at the *Eco*RI site, and the 247-bp fragment was isolated. Lanes: 1, control DNA (67,000 cpm); 2, 0.54 μg of pp32 (78,200 cpm); 3, 1.08 μg of pp32 (72,100 cpm); 4, 1.62 μg of pp32 (71,300 cpm); 5, 2.16 μg of pp32 (70,200 cpm); 6, G+A markers (35,600 cpm); 7, C+T markers (35,900 cpm). The gel was exposed for 8 days. The asterisk indicates the position of the nick adjacent to the circle junction (C.J.) site.

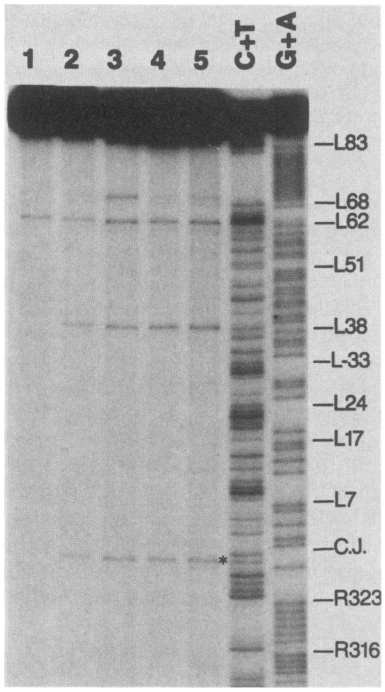

FIG. 2. Effect of varying AMV pp32 concentration on nicking within the Schmidt-Ruppin A RSV LTR region viral plus strand. Different amounts of AMV pp32 were incubated with 3 μg of pPvuII-DG at 37°C for 1 h; all reaction mixtures were adjusted to 32 mM NaCl. One-half of the sample was digested with *Eco*RI, 5′ end labeled, and then digested with *Sph*I. The 247-bp labeled fragment was isolated and analyzed by polyacrylamide gel electrophoresis under denaturing conditions. Lanes: 1, control DNA (67,900 cpm); 2, 0.54 μg of pp32 (63,850 cpm); 3, 1.08 μg of pp32 (62,660 cpm); 4, 1.62 μg of pp32 (67,370 cpm); 5, 2.16 μg of pp32 (68,955 cpm); 6, C+T markers (27,390 cpm); 7, G+A markers (28,920 cpm). The gel was exposed for 7 days. The asterisk identifies the position of the nick adjacent to the circle junction (C.J.) site. All counts are expressed as Cerenkov counts per minute.

What circle junction sequences or other LTR DNA sequences are necessary for integration of supercoiled viral DNA in vivo? Panganiban and Temin (18) have demonstrated (i) that 5 to 12 bp at the U_3 end and 6 to 9 bp at the U_5 end of the spleen necrosis virus LTR are required for integration and (ii) that a small restriction fragment (49 bp) containing the spleen necrosis virus circle junction region, when inserted in the *gag* region, can serve as an attachment site to host DNA (20). Recently, Colicelli and Goff (1) confirmed these results with murine leukemia retrovirus. By using circle junction deletion mutants, the inverted repeat at the LTR boundary was shown to be required for the establishment of proviral DNA and for productive infection. These data suggest that there are minimal sequences required in the circle junction region for the integration of viral DNA.

The distance between the two cleavage sites at the circle junction can be changed without altering the sequence specificity of cleavage. These cleavage sites are maintained even if the distance between the two sites is increased from 4 to 5 bp, as in the case of the pA043 clone of viral DNA (Fig. 5). Here, cleavage at the conserved CA and AC dinucleotides would lead to a 5-base rather than a 4-base overhang. A similar argument can be used to explain the results of Colicelli and Goff (1). In analyzing autointegrants of a mutant murine leukemia retrovirus clone that was missing 1

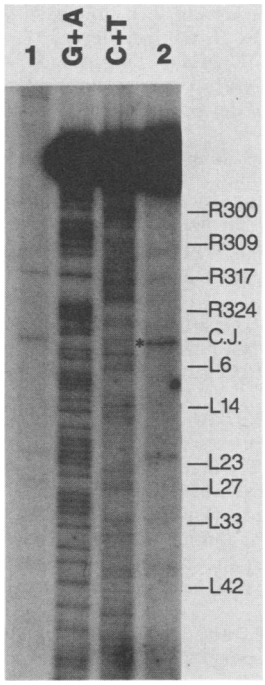

FIG. 4. Defining frequencies of cleavage at the four major sites of nicking by AMV pp32 on the Schmidt-Ruppin A RSV LTR circle junction (C.J.) region. pPvuII-DG DNA (1.5 μg) was nicked by pp32 at a protein-DNA ratio of 88:1. The DNA was then digested with *Eco*RI and 5′ end labeled. The 330-bp doubly end labeled DNA fragment was isolated, and most of the fragment was subsequently digested with *Hin*fI. The resulting 223-bp fragment, labeled only in the minus strand, was isolated and analyzed on a gel under denaturing conditions. Lanes: 1, 330-bp DNA fragment nicked by pp32 (the position of the full-length fragment is not shown; 25,300 cpm); G+A, G+A markers for the minus strand (37,000 cpm); C+T, C+T markers for minus strand (35,100 cpm); 2, analysis of 223-bp labeled *Eco*RI-to-*Hin*fI fragment (viral minus strand; 72,600 cpm). The gel was exposed for 7 days. The asterisk indicates the position of the nick adjacent to the C.J. site.

bp between the conserved CA and AC dinucleotides, they concluded that the circle junction had been cleaved at each dinucleotide, giving rise to a 3-base overhang. Thus, signals flanking the precise circle junction site may direct the cleavage to the conserved CA and AC sites.

Duyk et al. (5) have used deletion mutagenesis to define the sequences required for cleavage of a single-stranded DNA substrate by the αβ DNA polymerase-associated endonuclease. Their results indicate that the cleavage signals for the two strands are asymmetric with respect to the circle junction site. Cleavage of the minus strand requires a domain no larger than 44 nucleotides that spans the circle junction site. Cleavage of the plus strand requires no more than 22 nucleotides located entirely within the U_5 domain.

Duyk et al. (4) and Skalka et al. (24) have demonstrated that the αβ DNA polymerase in the presence of Mn^{2+} selectively nicks 3 nucleotides from the circle junction site on single-stranded or double-stranded DNA substrates. The AMV pp32 endonuclease in the presence of Mg^{2+} generates nicks on the plus and minus strands, each 2 nucleotides from the circle junction site (9; this report). However, the pp32 protein, in the presence of Mn^{2+} (9) or at high protein concentration (Fig. 3 and 4), is also capable of generating nicks 2 or 3 nucleotides from the circle junction site. Also, under different assay conditions, nicks mapping 3 nucleotides from the circle junction site were observed with pp32 (5, 24). It therefore appears likely that the nuclease sites of αβ and pp32 are related but express distinct differences in specificity of cleavage.

We have previously suggested that the dimeric pp32 protein forms a nucleosomelike structure on LTR DNA including the circle junction region (16). This structure encompasses approximately 170 nucleotides that extend from the upstream promoter region in U_3 through U_5 and past the circle junction site into the adjacent U_3 for about 34 bp. At a low protein-DNA molar ratio (16:1), electron microscopy clearly demonstrates the presence of visible pp32 protein complexes (approximately 8 to 35 nm in size) on supercoiled, open circular, or linear DNA molecules (D. P. Grandgenett, unpublished data). Taken together, these data suggest that the pp32 endonuclease may form a complex at the circle junction in vivo but that other LTR DNA sequences may also play a *cis* role in the regulation of pp32 functions. The pp32 DNA binding protein is located in the virion core structure (10) and, assuming that the p35 protein identified in AMV cores (25) is the pp32 DNA endonuclease, it is apparent that the number of pp32 single-chain molecules (140) per core structure is sufficient to permit formation of a major pp32-DNA protein complex in vivo. Conceivably, such a complex of viral protein(s) and

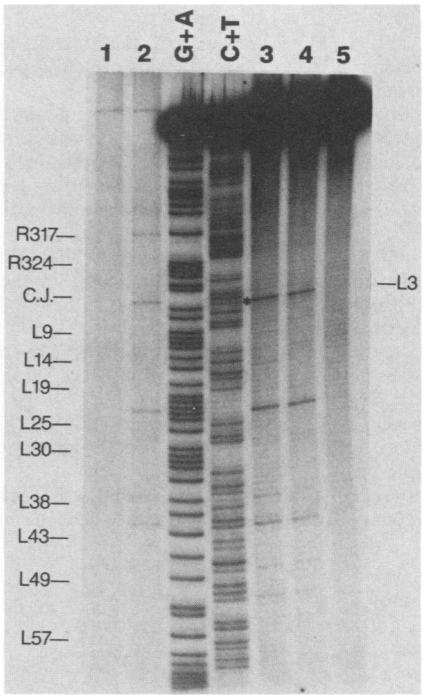

FIG. 5. Generation of a 5-bp staggered nick at the circle junction (C.J.) of pA043 by pp32. Supercoiled pA043 containing the LTR *Eco*RI fragment (3 μg) was nicked by pp32 under standard conditions. The DNA was processed as described in the legend to Fig. 4. Lanes: 1, control 331-bp *Eco*RI-generated DNA fragment (107,800 cpm); 2, 331-bp *Eco*RI DNA fragment nicked with 1.08 μg of pp32 (98,200 cpm); G+A, G+A markers for the minus strand (31,700 cpm); C+T, C+T markers for the minus strand (29,760 cpm); 3, *Eco*RI-to-*Hin*fI 224-bp fragment nicked with 1.08 μg of pp32 (104,000 cpm); 4, 0.54 μg of pp32 (98,200 cpm); 5, control *Eco*RI-to-*Hin*fI DNA fragment (96,600 cpm). The gel was exposed for 16 days. The asterisk indicates the position of the nick adjacent to the C.J. site.

supercoiled viral DNA could be the immediate precursor to integrated DNA. In this setting, the viral endonuclease may function, cleaving viral and perhaps cellular DNA during the integration reaction.

This work was supported by Public Health Service grants CA 16312 (D.P.G.) and CA 33147 (R.S.) from the National Institutes of Health. J.O. is a fellow of the Leukemia Society of America.

We thank Norma C. Urani for typing the manuscript.

LITERATURE CITED

1. **Colicelli, J., and S. P. Goff.** 1985. Mutants and pseudorevertants of Moloney murine leukemia virus with alterations at the integration site. Cell **42**:573–580.
2. **Copeland, T. D., D. P. Grandgenett, and S. Oroszlan.** 1980. Amino acid sequence analysis of reverse transcriptase subunits from avian myeloblastosis virus. J. Virol. **36**:115–119.
3. **Donehower, L. A., and H. E. Varmus.** 1984. A mutant murine leukemia virus with a single missense codon in *pol* is defective in a function affecting integration. Proc. Natl. Acad. Sci. USA **81**:6461–6465.
4. **Duyk, G., J. Leis, M. Longiaru, and A. Skalka.** 1983. Selective cleavage of the avian retrovirus LTR sequence by the endonuclease associated with the αβ form of the avian reverse transcriptase. Proc. Natl. Acad. Sci. USA **80**:6745–6749.
5. **Duyk, G., M. Longiaru, D. Cobrinik, R. Kowal, P. DeHaseth, A. M. Skalka, and J. Leis.** 1985. Circles with two tandem long terminal repeats are specifically cleaved by *pol* gene-associated endonuclease from avian sarcoma and leukosis viruses: nucleotide sequences required for site-specific cleavage. J. Virol. **56**:589–599.
6. **Eisenman, R. N., W. S. Mason, and M. Linial.** 1980. Synthesis and processing of polymerase proteins of wild-type and mutant avian retroviruses. J. Virol. **36**:62–78.
7. **Golomb, M., and D. P. Grandgenett.** 1979. Endonuclease activity of purified RNA-directed DNA polymerase from avian myeloblastosis virus. J. Biol. Chem. **254**:1606–1613.
8. **Golomb, M., D. P. Grandgenett, and W. Mason.** 1981. Virus-coded DNA endonuclease from avian retrovirus. J. Virol. **38**:548–555.
9. **Grandgenett, D. P., and A. C. Vora.** 1985. Site-specific nicking at the avian retrovirus LTR circle junction by the viral pp32 DNA endonuclease. Nucleic Acids Res. **13**:6205–6221.
10. **Grandgenett, D. P., A. C. Vora, and R. D. Schiff.** 1978. A 32,000-dalton nucleic acid-binding protein from avian retrovirus cores possesses DNA endonuclease activity. Virology **89**:119–132.
11. **Hippenmeyer, P. J., and D. P. Grandgenett.** 1984. Requirement of the avian retrovirus pp32 DNA binding protein domain for replication. Virology **137**:358–370.
12. **Hippenmeyer, P. J., and D. P. Grandgenett.** 1985. Mutants of the Rous sarcoma virus reverse transcriptase gene are nondefective in early replication events. J. Biol. Chem. **260**:8250–8256.
13. **Knaus, R. J., P. J. Hippenmeyer, T. K. Misra, D. P. Grandgenett, V. R. Müller, and W. M. Fitch.** 1984. Avian retrovirus pp32 DNA binding protein. Preferential binding to the promoter region of the long terminal repeat DNA. Biochemistry **23**:350–359.
14. **Leis, J., G. Duyk, S. Johnson, M. Longiaru, and A. Skalka.** 1983. Mechanisms of action of the endonuclease associated with the αβ and ββ forms of avian RNA tumor virus reverse transcriptase. J. Virol. **45**:727–739.
15. **Maxam, A. M., and W. Gilbert.** 1980. Sequencing end-labeled DNA with base-specific chemical reactions. Methods Enzymol. **65**:499–560.
16. **Misra, T. K., D. P. Grandgenett, and J. T. Parsons.** 1982. Avian retrovirus pp32 DNA-binding protein. I. Recognition of specific sequences on retrovirus DNA terminal repeats. J. Virol. **44**:330–343.
17. **Olsen, J. C., and R. Swanstrom.** 1985. A new pathway in the generation of defective retrovirus DNA. J. Virol. **56**:779–789.
18. **Panganiban, A. T., and H. M. Temin.** 1983. The terminal nucleotides of retrovirus DNA are required for integration but not virus production. Nature (London) **306**:155–158.
19. **Panganiban, A. T., and H. M. Temin.** 1984. The retrovirus *pol* gene encodes a product required for DNA integration: identification of a retrovirus *int* locus. Proc. Natl. Acad. Sci. USA **81**:7885–7889.
20. **Panganiban, A. T., and H. M. Temin.** 1984. Circles with two tandem LTRs are precursors to integrated retrovirus DNA. Cell **36**:673–679.
21. **Samuel, K. P., T. K. Papas, and J. C. Chirikjian.** 1979. DNA endonuclease associated with the avian myeloblastosis virus DNA polymerase. Proc. Natl. Acad. Sci. USA **76**:2659–2663.
22. **Schiff, R. D., and D. P. Grandgenett.** 1980. Partial phosphorylation in vivo of the avian retrovirus pp32 DNA endonuclease. J. Virol. **36**:889–893.
23. **Schwartzberg, P. J., J. Colicelli, and S. P. Goff.** 1984. Construction and analysis of deletion mutations in the *pol* gene of Moloney murine leukemia virus: a new viral function required for establishment of the integrated provirus. Cell **37**:1043–1052.
24. **Skalka, A. M., G. Duyk, M. Longiaru, P. DeHaseth, R. Terry, and J. Leis.** 1984. Integrative recombination—a role for the retroviral reverse transcriptase. Cold Spring Harbor Symp. Quant. Biol. **49**:651–659.
25. **Stromberg, K., N. E. Hurley, N. L. Davis, R. R. Rueckert, and E. Fleissner.** 1974. Structural studies of avian myeloblastosis virus: comparison of polypeptides in virion and core component by dodecyl sulfate-polyacrylamide gel electrophoresis. J. Virol. **13**:513–528.
26. **Swanstrom, R., W. J. DeLorde, J. M. Bishop, and H. E. Varmus.** 1981. Nucleotide sequence of cloned unintegrated avian sarcoma virus DNA: viral DNA contains direct and inverted repeats similar to those in transposable elements. Proc. Natl. Acad. Sci. USA **78**:124–128.